

The Composition of RR Lyrae Stars: Start-line for the AGB

George Wallerstein and Wenjin Huang

Department of Astronomy, University of Washington
Box 351580, Seattle, WA 98195
wall@astro.washington.edu; hwenjin@astro.washington.edu

Abstract. This paper summarizes research on abundances in RR Lyrae stars that one of us (GW) has been engaged in with various astronomers. In addition we report on preliminary analysis of the abundances of C, Si, S and Fe in 24 RR Lyrae stars. Our model atmosphere analysis, including NLTE effects, are based on the spectra of resolving power 30,000 obtained at the Apache Point Observatory.

1. Introduction

This paper reports on research by Sergei M. Andrievsky, Valentin V. Kovtyukh, Marcio Catelan, Dana Casetti-Dinescu, and Gisella Clementini as well as ourselves.

The RR Lyrae stars are of great value in studies of the structure of our Galaxy and the history of its composition as modified by stellar nucleosynthesis over the ages. The fact that they show a narrow range of luminosity from about $M_V=0.4$ to 0.8, as derived from their membership in globular clusters, allows their distances to be derived and their orbits calculated from their proper motions and radial velocities. Their effective temperatures vary from approximately 6000 to 7000 K during their pulsation. Their spectra often show lines of many elements without excessive blending.

The chemical composition of RR Lyrae stars is a combination of their original composition when they were main sequence stars near $M_V=4.5$ with important changes induced by nuclear reactions whose products may be convected to the stellar sur-

face. The first mixing event to affect their atmospheres is the deepening of convection as the star leaves the subgiant branch and begins its evolution up the almost vertical giant branch (Hoyle & Schwarzschild 1955). CNO-processing converts some carbon into nitrogen and reduces the $^{12}\text{C}/^{13}\text{C}$ ratio from its initial value to about 20. As the star's evolution slows down at the red giant clump additional mixing further reduces the carbon and lowers the $^{12}\text{C}/^{13}\text{C}$ ratio to about 4-8 (Gilroy & Brown 1991; Charbonnel 1994; Charbonnel, Brown, & Wallerstein 1998). These changes have been seen in many globular clusters.

At the tip of the red giant branch important events take place. The triple-alpha reaction starts in the degenerate core producing additional carbon. At first the temperature rises exponentially because the pressure and density do not respond until the degeneracy is removed by the temperature rise and the reaction rate depends approximately on the temperature raised to the 30th power. This sets up a grossly

superadiabatic temperature gradient and initiates violent convection (Mocák et al. 2009). Calculations indicate that the products of helium burning do not reach the surface but observations of the carbon abundance in RR Lyrae stars are useful to confirm the accuracy of the calculations and to describe the initial conditions for stars that will eventually evolve up the AGB, perhaps to become carbon stars. In addition mass-loss on the red giant branch plus additional mass-loss at the time of the helium-flash reduces the stellar mass from its original value of about 0.8 Msun to about 0.55 Msun as derived from multi-periodic RR Lyrae stars. Such mass-loss may give us a glimpse into the interior of what had once been a red giant.

Our first project to determine the composition of RR Lyrae stars was suggested by M. Catelan who noted that a few RR Lyrae and related stars showed kinematics similar to that of Omega Cen. The first is VY Ser, a genuine RR Lyrae star of period 0.714 days, while 2 more, V716 Oph and XX Vir have periods slightly longer than 1.0 days and are usually called short-period type II cepheids, but might be referred to as long-period RR Lyrae stars. Dana Casetti-Dinescu confirmed that their galactic orbits do indeed relate them to Omega Cen. The period of VY Ser is typical of RR Lyrae stars in Omega Cen, but only 7 short-period cepheids are known in Omega Cen (Clement et al. 2001). In fact it is remarkable that astronomers have defined the break between RR Lyraes and short period cepheid to equal to the period of rotation of the earth. Our observations consisted of 4 echelle spectra of VY Ser, 5 of V716 Oph, and 2 of XX Vir that have been analysed by Andrievsky and Kovtyukh. All 3 stars show $[Fe/H]$ close to -1.6 which is typical of Omega Cen but cannot be used to reveal the strong gradient of $[s/Fe]$ when plotted against $[Fe/H]$ in Omega Cen (Vanture, Wallerstein, & Brown 1994; Norris & Da Costa 1995).

Our second group of targets was RR Lyrae stars with period greater than

0.75 days. Such stars are very rare in globular clusters with the conspicuous exception of the two unusual clusters, NGC 6388 and 6441 (Pritzl et al. 2001, 2002). These relatively metal rich clusters with $[Fe/H]$ near -0.8 have numerous long-period RR Lyrae stars. In the general field such stars are rare but some are known and their light curves have been obtained by Schmidt (2002). Only a few are sufficiently bright for highres spectroscopy with the 3.5-m telescope of the Apache Point Observatory. They are listed in Wallerstein, Kovtyukh, & Andrievsky (2009). $[Fe/H]$ values were found for 4 stars but their metallicities ranged from -1.8 to $+0.2$. Hence our analyses of these stars failed to relate them to NGC 6388 and 6441. KP Cyg remains an almost unique RR Lyrae star with a period of 0.856 days and $[Fe/H] = +0.2$ on the basis of 5 spectra well distributed in phase. It had already been recognized as having $\delta-S = 0$ by Preston (1959). Our spectra show a typical velocity curve for an RR Lyrae star with H-alpha emission at phases 0.43, 0.72, and 0.80.

The third aspect of our RR Lyrae analyses was the recognition that the relatively metal-rich stars show an apparant excess of carbon (Wallerstein, Kovtyukh, & Andrievsky 2009)). The carbon abundance was derived from the lines around 7115\AA of multiplets 108 and 109 of Wiese, Fuhr, & Deters (1998). These lines are sufficiently weak to be found only in stars with $[Fe/H] > -1.0$. For metal-poor stars stronger lines must be employed which suffer from NLTE (Fabbian et al. 2006). Fabbian has told us (private communication) that the lines around 7115\AA should not suffer from significant NLTE effects. The best strong lines are one at 8335\AA and from multiplet 62 beyond 9000\AA . That spectral region contains many moderately strong atmospheric H_2O lines.

2. Observation and Data Reduction

New Observations were obtained with the echelle spectrograph on the Apache Point 3.5-m telescope in March, November and December, 2009. The resolving power is about 30,000 and the signal-to-noise ratio of the reduced spectra is usually 100-150. The cold temperatures and altitude of 9200 ft permit very effective division by the spectrum of a hot rapidly rotating star so as to cancel out the atmospheric H₂O absorption lines, especially beyond 8900Å. We have used the H γ line to establish Teff and the known mass and luminosity of the RR Lyrae stars for the derivation of the surface gravity (without introducing the perturbation of log g by the acceleration induced by pulsation). In addition to deriving the iron abundance from Fe II lines we have compared the C I lines with lines of S I whose excitation and ionization potentials are similar to those of C I. We added Si II to the data base as a check on the alpha element excess usually seen in metal-poor stars. The observed lines and their atomic properties are shown in Table 1. The abundances were derived using the updated version of the line synthesis code, MOOG, with the Kurucz atmosphere models (Castelli & Kurucz 2004). In Table 2 we show the derived abundances of C, S, Si, and Fe. We also show the Delta-S value from Preston (1959) or other sources such as Layden (1994). The correlation of the Fe abundance with delta-S is very good.

3. Results

In Fig. 1(a) we show [Si/Fe] plotted against [Fe/H]. The pattern is similar to that which is usually found for metal-poor stars. In Fig. 1(b) the behavior of [S/Fe] is qualitatively similar to that of [Si/Fe] but is displaced downward by about 0.4 dex. We do not fully understand the low [S/Fe] values because we have already applied the NLTE corrections of Takeda et al. (2005) to the derived sulfur abundance. Fig. 1(c) shows [C/Fe] vs. [Fe/H] for these stars. The

scatter is unfortunately large possibly because we have ignored the pulsation effect on log g . However, in Fig. 1(c), it is evident that relatively high carbon abundances appear in the high [Fe/H] region. Note that we also used the NLTE corrections of Fabbian et al. (2006) in our carbon abundance calculations. Since both the ionization potential and the excitation potentials of the lines are similar, the effects of log g and possible NLTE uncertainties should be diminished in the abundance ratios of [C/S] and [C/Si]. In Fig. 1(d), a clear trend of increasing [C/S] is present. The same trend is seen even more clearly in the plot of [C/Si] vs. [Fe/H] (Fig. 1(e)). The Si abundances come from the ionized lines of similar excitation to the C I lines (see Table 1).

Acknowledgements. We are grateful to Damian Fabbian and Elisabetta Caffau for helpful advice regarding NLTE in C I and S I, and to Sergei Andrievsky for helpful suggestions. This research was supported by the Kenilworth Fund of the New York Community Trust.

References

- Castelli, F., & Kurucz, R. L. 2004, *astro-ph/0405087*
- Charbonnel, C. 1994, *A&A*, 282, 811
- Charbonnel, C., Brown, J. A., & Wallerstein, G. 1998, *A&A*, 332, 204
- Clement, C. M. et al. 2001, *AJ*, 122, 2587
- Fabbian, D., Asplund, M., Carlsson, M., & Kiselman, D. 2006, *A&A*, 458, 899
- Gilroy, K. K., & Brown, J. A. 1991, *ApJ*, 371, 578
- Hoyle, F., & Schwarzschild, M. 1955, *ApJS*, 2, 1
- Layden, A. C. 1994, *AJ*, 108, 1016
- Mocák, M., Müller, E., Weiss, A., & Kifonidis, K. 2009, *A&A*, 501, 659
- Norris, J. E., & Da Costa, G. S. 1995, *ApJ*, 447, 680
- Preston, G. W. 1959, *ApJ*, 130, 507
- Pritzl, B. J., Smith, H. A., Catelan, M., & Sweigart, A. V. 2001, *AJ*, 122, 2600

Table 1. Observed lines

Wavelength (Å)	Ions	χ (eV)	$\log gf$
4932.05	6.00	7.68	-1.658
5052.17	6.00	7.68	-1.303
5380.34	6.00	7.68	-1.616
7111.47	6.00	8.63	-1.085
7113.18	6.00	8.64	-0.773
7115.17	6.00	8.63	-0.824
7116.99	6.00	8.64	-0.907
7119.66	6.00	8.63	-1.148
8335.15	6.00	7.68	-0.437
9061.44	6.00	7.47	-0.347
9062.49	6.00	7.47	-0.455
9078.29	6.00	7.47	-0.581
9088.51	6.00	7.47	-0.430
9094.83	6.00	7.48	0.151
9111.81	6.00	7.48	-0.297
9405.73	6.00	7.68	0.286
3853.66	14.01	6.86	-1.341
5957.56	14.01	10.07	-0.225
5978.93	14.01	10.07	0.084
6347.09	14.01	8.12	0.149
6371.36	14.01	8.12	-0.082
8694.70	16.00	7.87	0.154
9212.91	16.00	6.52	0.430
9237.54	16.00	6.52	0.030

Pritzl, B. J., — 2002, AJ, 124, 949

Schmidt, E. G. 2002, AJ, 123, 965

Takeda, Y. et al. 2005, PASJ, 57, 751

Vanture, A. D., Wallerstein, G., & Brown,
J. A. 1994, PASP, 106, 835

Wallerstein, G., Kovtyukh, V. V., &
Andrievsky, S. M. 2009, ApJ, 692, 127

Wiese, W. L., Fuhr, J. R., & Deters, T. M.
1998, NIST Monograph No. 7

Table 2. Abundances of Observed RR Lyrae Stars

Star	$P(\text{days})$	$T_{\text{eff}}/\log g/V_t$	ΔS	[Fe/H]	[C/Fe]	[S/Fe]	[Si/Fe]	[C/S]	[C/Si]	Note
V445OPH	0.397	6500/2.5/2.2	1	0.24	-0.39	-0.22	-0.07	-0.17	-0.32	1,3
RRGEM	0.397	6750/2.5/3.1	3	0.01	-0.39	-0.44	-0.20	0.05	-0.19	1,3
SWAND	0.442	6500/2.5/4.0	0	-0.16	-0.39	-0.56	-0.06	0.17	-0.33	3
DXDEL	0.473	6500/2.5/3.1	2	-0.21	-0.28	-0.20	-0.18	-0.08	-0.10	1,3
ARPER	0.426	6500/2.5/4.0	0	-0.32	-0.32	-0.51	0.01	0.19	-0.33	3
KXLYR	0.441	7000/3.0/3.1	0	-0.57	-0.22	-0.27	0.35	0.05	-0.57	2,3
XZDRA	0.476	6500/2.5/3.0	3	-0.75	0.06	0.09	0.33	-0.03	-0.30	2,3
UU VIR	0.476	6250/2.5/3.2	2	-0.90	-0.42	0.11	0.52	-0.53	-0.94	
BHPEG	0.641	6500/2.5/2.2	6	-1.17	-0.53	0.10	0.40	-0.63	-0.93	
WCVN	0.552	6250/2.5/3.0	7	-1.22	-0.46	-0.01	0.42	-0.45	-0.88	
VZHER	0.440	6250/2.5/2.6	4	-1.30	-0.23	0.21	0.60	-0.44	-0.83	
RVUMA	0.468	6500/2.5/2.3	3.5	-1.31	-0.05	0.22	0.58	-0.27	-0.63	
RRLEO	0.452	6500/2.5/2.8	5	-1.39	-0.04	0.22	0.61	-0.26	-0.65	
TTLYN	0.597	6500/2.5/3.4	7	-1.41	-0.98	-0.24	0.12	-0.74	-1.10	
RRLyr	0.567	6500/2.5/4.0	6	-1.44	-0.91	-0.03	0.14	-0.88	-1.05	
TUUMA	0.558	6500/2.5/3.4	6	-1.46	-0.32	-0.04	0.69	-0.28	-1.01	
VXHER	0.455	6000/2.5/2.4	5	-1.48	-0.34	0.16	0.59	-0.50	-0.93	
DHPEG	0.256	6500/2.5/3.0	0	-1.53	-0.12	0.23	0.75	-0.35	-0.87	
RRCET	0.553	6500/2.5/3.7	5	-1.61	0.15	0.09	0.85	0.06	-0.70	
STBOO	0.622	6250/2.5/4.0	9	-1.77	-0.50	-0.15	0.46	-0.35	-0.96	
SVERI	0.714	6500/2.5/3.0	9	-1.94	-0.44	-0.15	0.12	-0.29	-0.56	
RUPSC	0.390	6500/2.5/3.5	7	-2.04	-0.62	-0.12	0.51	-0.50	-1.13	
RZCEP	0.511	6500/2.5/3.0	5	-2.10	-0.41	0.01	0.57	-0.42	-0.98	
XARI	0.651	6250/2.5/3.8	10	-2.68	< -0.46	0.01	0.55	< -0.47	< -1.01	

1. Si II 5957, 5978 only
2. Si II 3853, 5957, 5978 only
3. C I 7100 lines only

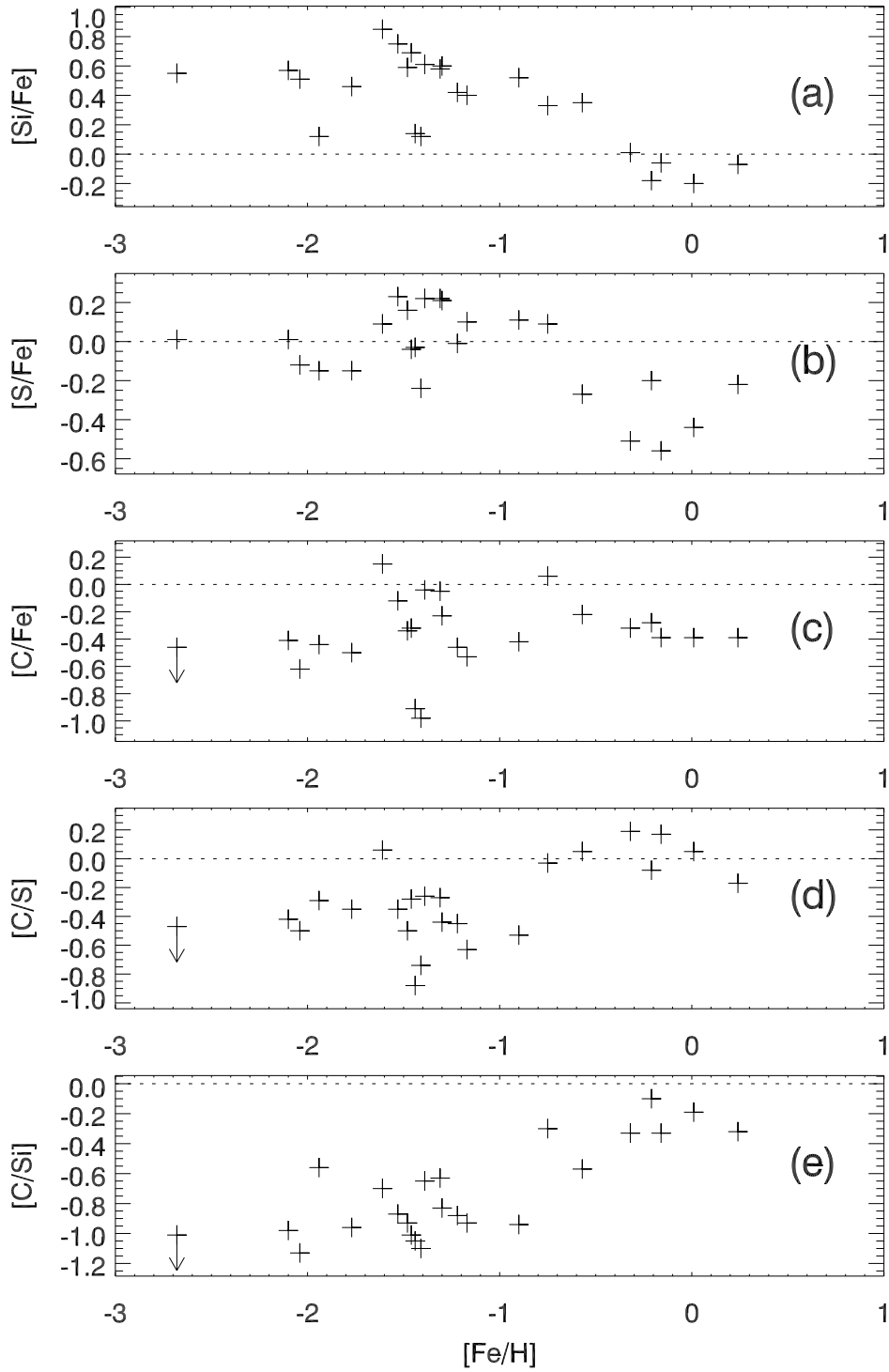


Fig. 1. Plots of abundance ratios versus $[\text{Fe}/\text{H}]$ based on Table 2: (a) Our derived $[\text{Si}/\text{Fe}]$ ratios based on ionized lines of both elements; (b) Our derived $[\text{S}/\text{Fe}]$ ratios based on S I and Fe II lines; (c) Our derived $[\text{C}/\text{Fe}]$ ratios based on C I and Fe II lines; (d) Our derived $[\text{C}/\text{S}]$ ratios based on C I and S I lines; (e) Our derived $[\text{C}/\text{Si}]$ ratios based on C I and Si II lines.